Spatial transcriptomics and in silico random pooling identify novel dopamine neuron subtype markers

Julio Aguila[1,#] Shangli Cheng[2,3#], Nigel Kee[1], Ming Cao[1], Qiaolin Deng[2,3*] and Eva Hedlund[1,*]
[1] Department of Neuroscience, Karolinska Institutet, Stockholm, Sweden
[2] Department of Physiology and Pharmacology, Karolinska Institutet, Stockholm, Sweden
[3] Center for Molecular Medicine, Karolinska University Hospital
[#]Equal contribution
[*]Correspondence: eva.hedlund@ki.se or qiaolin.deng@ki.se

Defining the transcriptional profiles of substantia nigra pars compacta and ventral tegmental area dopamine neurons may reveal mechanisms underlying their differential vulnerabilities in Parkinson's disease. Existing studies display extensive variability due to small sample sizes, resulting in troublingly few reproducible subtype-specific markers. We combine spatial transcriptomics (LCM-seq) on human tissue with an iterative, random pooling algorithm, that reveal novel genes which robustly identify dopamine neuron subtypes across species.

Midbrain dopamine neurons are divided into two major subpopulations, the substantia nigra pars compacta (SNc) and the ventral tegmental area (VTA). SNc dopamine neurons project to the dorsolateral striatum and are severely affected in Parkinson's Disease (PD). VTA dopamine neurons project to cortical and mesolimbic areas and are more resilient to degeneration. These subtypes have been extensively investigated in numerous models towards the goal of identifying molecular mechanisms that can prevent degeneration or to model disease. As SNc dopamine neurons represent the ideal cell type for transplantation in PD[1-3], a targeted and thorough transcriptional profiling will serve as a foundation for their *in vitro* derivation. When we revisit previous publications addressing the identity of VTA and SNc midbrain dopamine neurons in mouse and rat[4-8], we find that a surprisingly low fraction of differentially expressed genes (DEGs) are common to all studies (Supplementary Tables 1 and 3 and Supplementary Fig. 1a,b). Cross-comparison of these genes with our previously published human dataset[9] (Supplementary Tables 1 and 3), identify overlap only of SOX6 and CALB1 across SNc and VTA gene lists, respectively (Supplementary Fig. 1c). These discrepancies highlight the urgent need for a more thorough investigation into VTA and SNc identity across different species, with particular focus on the adult human brain.

Previously, we have applied the highly sensitive spatial transcriptomic method LCM-seq in post mortem tissues from three female human subjects[9]. We have now expanded our analysis of dopamine neurons individually isolated from SNc and VTA, to include an additional 18 adult male human subjects (Supplementary Fig. 2a-h, Supplementary Table 2). DESEq2 analysis, considering the latter 18 male subjects, identified 74 differentially expressed genes (DEGs) (Supplementary Table 4), which hierarchically resolved SNc from VTA neurons (Fig. 1a).

Reassuringly, these genes also distinguished SNc and VTA samples from our previous study of three female subjects[9] (Fig. 1b). However, given the little overlap with our previously published DEG list we compared the resolutive power of the 74 DEGs with that of the 100 DEGs identified using a small cohort of only three female subjects (published in Nichterwitz et al.) (Supplementary Fig. 2i, Supplementary Table 5). Notably, the 100 previously identified DEGs fully resolved the SNc and VTA of the small Nichterwitz et al. cohort, but were not as robust in separating the 18 male subjects (Supplementary Fig. 2i-j). Moreover, when DEGs from the two datasets were compared (Fig. 1c), only 7 and 21 genes overlapped in SNc and VTA gene lists, respectively. This discrepancy highlights the difficulty in analyzing transcriptome data from small cohorts of human subjects that were likely confounded by individual variations. Consequently, subsets of lineage-specific markers may fall into significance depending on the size of different cohorts, resulting in potentially few commonly shared genes across the groups.

To address this problem, we designed a random pooling algorithm (Fig. 1d, see methods), available at https://github.com/shanglicheng/RandomPooling, that iteratively samples an increasing proportion of a cohort of subjects, while performing DESeq2 analysis at each iteration. Upon completion, genes are ranked according to the cumulative frequency that they were scored as differentially expressed, as a function of sample size. To reduce the individual variability, we selected 12 subjects from our cohort from which both SNc and VTA samples were available. Application of this random pooling strategy to these 24 samples yielded frequency ranks of DEGs for SNc and VTA (Supplementary Fig. 2k-l, Supplementary Table 6) that included many existing human and/or rodent SNc and VTA markers[4-12] (Supplementary Table 3). We then designated genes within the top 30% of the most frequent genes' score, as "stable DEGs". This resulted in eight genes for the SNc (Fig. 1e, Supplementary Table 6) and 25 genes for the VTA (Fig. 1f, Supplementary Table 6). Importantly, many of the stable genes (labeled in red***** for SNc and blue***** for VTA) were among the aforementioned overlapping DEGs (Fig. 1c). Notably, these genes became stably differentially expressed only as at least eight subjects were included in the random pooling strategy (Fig. 1e,f), suggesting this to be roughly the minimal cohort size required to distinguish these two closely related subpopulations. The expression of SNc stable genes was validated in two independent human microarray datasets[10,12] (which lacked VTA samples for comparison) (Supplementary Fig. 2m). Finally, these 33 stable genes faithfully classified all 18 male subjects from our current dataset together with three female subjects investigated previously[9] (Fig. 1g). Moreover, these samples represent the largest human dataset profiling of SNc and VTA dopamine neurons to date.

To investigate cross-species similarities, we applied our random pooling algorithm to an adult mouse single-cell dataset[8](Supplementary Fig. 3a-c). Single cells from all postnatal ages were initially assessed for expression of known dopamine neuron markers (Supplementary Fig. 3a,b) prior to iterative random pooling and differential gene expression analysis (Supplementary Fig. 3c). We identified 35 stable SNc genes and 53 stable VTA genes (Fig. 2a,b, Supplementary

Table 7). These 88 genes effectively classified all single cells into their correct subtype (Supplementary Fig. 3d). Several stable genes for SNc and VTA were novel, while others were previously described[4-8,11] (Supplementary Fig. 3e,f, red labels). Some markers previously reported as differentially expressed[4-8,11] ranked just below our 30% frequency cutoff and were thus not designated as stable (Fig. 3e,f, black labels).

We next investigated the overlap between our human and mouse stable genes (Fig. 2c). Two genes, ZCCHC12 and CDH13, were common to human and mouse VTA. A third gene SERPINE2, was expressed in human VTA, while it's mouse homolog Serpine2, was expressed in the mouse SNc. To investigate the predictive power of these three common genes, we established a workflow whereby samples would be hierarchically clustered, and then scored for accuracy, according to the percentage of samples that were correctly classified, such that 100% reflects perfect accuracy, and 50% reflects a random outcome (see methods). Further, this was performed with either the full list of stable genes, or excluding the three common genes, on either human and mouse samples (Fig. 2d-l). As expected, when using a complete stable gene list to resolve samples within that same species, negligible reduction in the accuracy was observed after removal of the three common genes in either mouse (Fig. 2d,e) or human (Fig. 2i,j). Surprisingly, despite their poor overlap, both species' stable genes could moderately separate the other species (Fig. 2f,k). However, subsequent exclusion of the three common genes led to a dramatic reduction in accuracy (Fig. 2g,l). This was most pronounced when mouse-specific stable genes (i.e. excluding Zcchc12, Cdh13 and Serpin2) were used to resolve human samples, resulting in a significant decreased accuracy of 56.76%, (Fig. 2l), versus 72.02% for human-specific stable genes (i.e. excluding ZCCHC12, CDH13 and SERPIN2) applied to mouse samples (Fig. 2g). These results highlight the significant predictive power of these three common genes, which alone could accurately classify SNc or VTA samples in either species (Fig. 2h,m).

The low fraction of common genes may be due to non-overlapping stable genes (43 for SNc, and 73 for VTA, Fig. 2c) falling outside the specified 30% frequency threshold. Thus, using this same exclusion paradigm, we calculated the accuracy to resolve cross-species SNc and VTA samples upon random exclusion of any three stable genes (see methods, Fig. 3a and Supplementary Fig. 4a). Briefly, scores were determined for each stable gene by calculating the mean decrease in accuracy following exclusion of the given stable gene together with any two other stable genes. Previous exclusion of CDH13, ZCCHC12 and SERPINE2 from the human stable list reduced the accuracy in classifying mouse samples from 84.36% to 72.02% (Fig. 2f,g), and in this new workflow SERPINE2 accordingly occupied the top rank, while ZCCHC12 and CDH13 occupied ranks 7 and 24 respectively (Fig. 3a). Given that previous exclusion of Cdh13, Zcchc12 and Serpine2 from the mouse stable list drastically reduced the accuracy in resolving human samples (from 86.41% to 56.76%, Fig. 2k,l), it was not unexpected that these three common genes occupied the very top ranks (1, 4 and 6 respectively) (Supplementary Fig. 4a). These genes also displayed definitive expression patterns in adult mouse (Figure 3b, P56, Allen Institute for Brain Science, available from http://developingmouse.brain-map.org). Exclusion of

other human stable genes could also impair classification accuracy of mouse samples, including, FXYD6, GSGL1, ATP2A3, NECAB1, and LY6H (Fig. 3a,c). Using immunohistochemistry in human post mortem tissue (Supplementary Table 8), we confirmed differential gene expression at the protein level for the human stable genes ATP2A3 and CRYM (Fig. 3d).

Moreover, further investigation of the mouse stable lists revealed that Calb1, an established VTA marker in both mouse[5,7,8] (Fig. 3c) and human[9] (Fig. 3d), strongly contributed to the separation of human samples (Supplementary Fig. 4a). In line with this, its' rank on the human VTA list was close to the 30% frequency threshold (Supplementary Fig. 2l). Other mouse stable genes, whose exclusion mildly impaired classification of human samples, also fell just outside the 30% frequency threshold for human stable genes (e.g. Slc1a2, Maoa, Tppp3, Lix1, Adrbk2) (Supplementary Fig. 2k,l). *In situ* analysis of these genes in adult mouse was consistent with their differential enrichment in human samples (Supplementary Fig. 4b,c, green labels). Finally, many novel mouse stable genes that had little impact on classification of human samples, also displayed expression patterns in line with their membership to either the SNc or VTA mouse stable gene lists (Supplementary Fig4. b,c, black labels).

In summary, we have used spatial transcriptomics with a novel random pooling algorithm that enabled us to derive robust and unique lists of SNc and VTA markers for both human and mouse. Interestingly, we find that only three genes are equally and strongly predictive across the two species. This highlights the vital need to appreciate the human marker profiles of these clinically relevant and highly similar dopaminergic sub-lineages. Such profiles will be invaluable for *in vitro* modeling of selective vulnerability, as well as for the derivation of authentic SNc neurons for use in cell transplantation strategies targeting Parkinson's disease.

Methods

Methods, including data availability, accession codes and references are available in the online version of the manuscript.

Acknowledgements

This work was funded by grants to E.H. from Parkinsonfonden (795/15; 910/16; 991/17); EU Joint Programme for Neurodegenerative Disease (JPND) (529-2014-7500); Swedish Medical Research Council (Vetenskapsrådet) (2016-02112); and NEURO Sweden; by grants to Q.D. from Swedish Research Council (Vetenskapsrådet) (2014-2870); Svenska Sällskapet för Medicinsk Forskning and Jeanssons Stiftelser; Åke Wiberg, Karolinska Institutets Forskningsstiftelser and Stiftelsen; by grants to J.A.B. from Karolinska Institutets Forskningsstiftelser and Stiftelsen för ålderssjukdomar (2014-2017). J.A.B. is supported by a postdoctoral fellowship from the Swedish Society for Medical Research and N.K. by a postdoctoral fellowship from Hjärnfonden, Sweden. Human post-mortem tissues were kindly received from the Netherlands Brain Bank (NBB) and the National Disease Research Interchange (NDRI).

Author contributions

E.H., Q.D. and J.A.B. conceived the project. J.A.B., S.C., Q.D. and E.H. designed experiments. J.A.B. and M.C. acquired data. J.A.B., S.C., N.K., Q.D. and E.H. analysed data. E.H. and Q.D. supervised the project. All authors co-wrote and gave critical input on the manuscript.

Competing interests

The authors declare no competing interests.

Online Methods

Ethics statement

We have ethical approval to work with human post-mortem samples (Supplementary Tables 2 and 9) from the regional ethical review board of Stockholm, Sweden (EPN 2012/111-31/1). Fresh frozen tissue or paraffin embedded samples were obtained through the National Disease Research Interchange (NDRI) or the Netherlands Brain Bank (NBB) with the written informed consent from the donors or the next of kin. The work with human tissues was carried out according to the Code of Ethics of the World Medical Association (Declaration of Helsinki).

Tissue sectioning

Sample preparation prior LCM-seq was carried out as follows. Frozen midbrain tissues obtained from the brain banks were attached to chucks using pre-cooled OCT embedding medium (Histolab). 10µm-thick coronal sections were acquired in a cryostat at -20 °C and placed onto precooled-PEN membrane glass slides (Zeiss). The slides with sections were kept at -20 °C during the sectioning and subsequently stored at -80 °C until further processed.

For immunohistochemistry, tissues from NDRI were fixed in PFA, cryoprotected by sequential gradients of sucrose (2%, 10%, 20% and 30%) and sectioned at 40µm on a freezing microtome. Tissues embedded in paraffin (NBB) were sectioned at 10µm on a sliding microtome. All tissue was subjected to antigen retrieval (0.01 M citric acid buffer, pH 6.0) for 20 min at 95 °C and treated to inactivate endogenous peroxidases (3% H_2O_2, 50% methanol in PBS) prior to staining.

LCM-seq

The laser capture procedure followed by sequencing library preparation was carried out as described[9,13].

Read mapping, gene expression quantification and quality control

Samples were sequenced using an Illumina HiSeq2000 or HiSeq2500 platform (reads of 43 or 50

bp in length respectively). The uniquely mapped reads were obtained by mapping to the human reference genome hg38/GRCh38 using STAR with default settings. The reads per kilobase of transcript per million mapped reads (RPKM) were estimated using ¨rpkmforgenes¨[14].

As part of the quality control we verified that samples had over 4.7±2.0 million reads and 10.5±1.1 kilo genes expressed with RPKM>1. Correlation across the samples was considered above 0.7. Additionally, we confirmed the expression on known midbrain dopamine neuron markers and the purity of each sample (see Supplementary Fig. 2h).

Differentially expressed analyses

Differentially expressed genes were identified using the R package ¨DESeq2¨ (current version: 1.16.1) where the cutoff for significance was an adjusted P value of 0.05. Identified DEGs (from different analysis and summarized below) are shown in Supplementary Tables 3 to 7.

Supplementary Table 3: Mouse differentially expressed genes[8]: 390 DEGs calculated from 73 SNc and 170 VTA cells.
Supplementary Table 4: Human differentially expressed genes (current study): 74 DEGs calculated from 16 SNc and 14 VTA samples from 18 male individuals.
Supplementary Table 5: Human differentially expressed genes[9]: 100 DEGs calculated from 4 SNc and 3 VTA samples from 3 female subjects.
Supplementary Table 6: Human stable genes: 33 DEGs calculated from 12 individuals (from the current study) using the random pooling algorithm.
Supplementary Table 7: Mouse stable genes: 88 DEGs calculated from 73 SNc and VTA cells[8] using the random pooling algorithm.

Random pooling algorithm

To counteract the variability among human subjects and identify the most reliable DEGs between SNc and VTA neurons across datasets we developed a random pooling algorithm (Fig. 1d and Supplementary Fig. 3c). The stable genes output of this analysis is correlated with the sample size and give an unbiased estimation of the number of individuals required to consistently distinguish these closely related subpopulations. Importantly this computational tool can be used for the comparison of any other two groups (https://github.com/shanglicheng/RandomPooling). In details:

1) Define ¨N¨ and ¨M¨ as the number of samples in Group 1 and Group 2, respectively.
2) Define ¨n¨ and ¨m¨ as the number of randomly selected samples from Group1 and Group2, where $n \in \{3, 4, 5, \ldots, N\}$ and $m \in \{3, 4, 5, \ldots, M\}$.
3) Pool ¨n¨ and ¨m¨ samples (temporary considered a ¨new data set¨) and calculate DEG.
4) Repeat steps 2) and 3) for ¨j¨ times (set to 1000 times in this study).

5) For every round, save the full list of DEGs, compute and rank their frequency.
6) Set a threshold (30% ratio in this study) to consider DEGs with higher frequency as stable genes.
Reliable genes appear when frequencies are above: Total times of random pooling x ratio (300 in this study). A stringent, but fair ratio can be defined by comparing the percentage of identified stable genes overlapping with the top 10%, 20%, 30% DEGs.

Random pooling applied to human samples
To reliable identify DEGs between human SNc and VTA samples, while minimizing subject variability, we selected 12 individuals (66% of the dataset) where both neuronal groups were available and sequenced. Hence, the number of randomly selected samples (¨n¨ and ¨m¨ from ¨i¨ individuals) was from three to 11 and the algorithm repeated 1000 times (Fig. 1d).

Random pooling applied to mouse single cells
For this adult mouse dataset (La Mano et. al, 2016) we defined the groups SNc (N=73 cells) and VTA (M=170 cells comprising VTA1, VTA2, VTA3 and VTA4). To compensate the unbalance in cell number and adjust dataset representation compared to the human analysis (66%, 12 out of 18 individuals), we first randomly collected a subset of 73 VTA cells, pairing both SNc and VTA. Similarly, the number of randomly selected samples (¨n¨ and ¨m¨ from ¨i¨ cells) was from 20 to 70 and the algorithm repeated again 1000 times (Supplementary Fig. 3c).

Accuracy calculation to distinguish SNc and VTA samples
To measure the power of stable genes in resolving SNc and VTA samples we calculated the accuracy. This is a quantitative parameter associated with correct group prediction using hierarchical clustering based on the first two dimensions (PC1 and PC2) of the PCA visualizing a given dataset. As we have two predicted groups (SNc and VTA), the minimum value for the accuracy is 50%. In details:

1) Define ¨N¨ and ¨M¨ as the total number of samples in Group 1 and Group 2, respectively.
2) Define ¨n¨ and ¨m¨ as the number of correctly predicted samples for Group1 and Group2, respectively.
3) Accuracy, expressed as percent, is calculated according to the formula:

Accuracy (%)= ((¨n¨+¨m¨)/(¨N¨+¨M¨)) * 100

We calculated the accuracy for six different conditions (stable gene sets) as follows:

a) Mouse stable genes applied to mouse (Fig. 2d) or human (Fig. 2k) samples.
b) Mouse stable genes excluding (Zcchc12, Cdh13, Serpine2) applied to mouse (Fig. 2e) or human (Fig. 2l) samples.

c) Human stable genes applied to mouse (Fig. 2f) or human (Fig. 2i) samples.
d) Human stable genes excluding (ZCCHC12, CDH13, SERPINE2) applied to mouse (Fig. 2g) or human (Fig. 2j) samples.
e) Mouse stable genes excluding three random markers applied to human samples (Supplementary Fig. 4a).
f) Human stable genes excluding three random markers applied to mouse samples (Fig. 3a).

To identify additional (but not common) stable genes from mouse or human with resolving power to the other species, we performed the above analysis **e)** and **f)**. Here we ranked the mean accuracy for a given stable gene upon random exclusion with any two others.

Immunohistochemistry of human tissues

We selected two human stable genes (ATP2A3 and CRYM) in addition to CALB1 to confirm their differential expression at the protein level with a peroxidase-based system[15]. Tissue sections in glass slides were blocked in PBS with 10% donkey serum and incubated with primary antibodies in 0.1% Triton X-100 in PBS with 10% donkey serum. Stainings against ATP2A3 (HPA007180, rabbit polyclonal, Sigma-Aldrich) or CRYM (HPA019086, rabbit polyclonal, Sigma-Aldrich) were carried out overnight at 4°C using 1 in 25 antibody dilution whereas CALB1 (1 in 300 dilution, mouse monoclonal, Swant) was detected after 48 h incubation at 4°C. Incubation with biotinylated secondary antibodies (1:300; Jackson Laboratories) were carried out for 3 h, followed by 1 h incubation in streptavidin–biotin complex (Vectastain ABC kit Elite, Vector Laboratories, Burlingame, CA, USA). Visualization was achieved after 10min incubation with 3,3'-diaminobenzidine solution (DAB, Vector Laboratories). Negative controls were performed for all stainings by omitting primary antibody. Cell nuclei were counterstained using Myers hematoxylin (Histolab) and tissue was dehydrated by sequential steps in increasing ethanol concentration and xylene prior preservation using coverslips with Mountex (Histolab).

Intensity measurements for quantification

For every staining, we imaged 5-7 random fields within the SNc and VTA regions. On average 203.33±35.63 cells were imaged per region and staining. Pictures were made at 40X magnification using bright-field of the Leica microscope DM6000/CTR6500 and DFC310 FX camera. The acquisition settings were optimized for each protein to avoid any saturation of signal, which could affect intensity calculations[16]. Intensity was measured by outlining individual SNc or VTA neurons and calculating average pixel intensity using ImageJ software (http://rsb.info.nih.gov/ij/). To correct for the background, three background intensity readings were taken per field. These readings were then averaged and substracted from the signal intensity within SNc or VTA neurons in the same area to give an accurate reading of protein staining

intensity. The signal intensity for a given protein was normalized to a value of one for the SNc or VTA (reference region), depending on the predicted preferential expression at the RNA level. Signal intensity for each protein was then compared to the reference region (value of one) to assess if the intensity was higher or lower. Investigators performing the intensity measurements and quantification of signal intensity were blinded to the target region (SNc and VTA) and protein staining.

Statistical analysis

For this study, statistical analyses were performed using ¨R¨. For the immunohistochemical analysis Mann-Whitney U test (¨wilcox.test¨ with alternative =¨two.sided¨ in the R function) was used to compare the mean intensity of ATP2A3, CRYM and CALB1 in the SNc and VTA. Individual statistical tests are detailed in the figure legends where significance is marked by $P < 0.05$. The number of subjects/cells used for each experiment is listed in the figure or figure legends. All results are expressed as mean ± SD.

Data availability

RNA sequencing data generated in this study have been submitted to the Gene Expression Omnibus (GEO) of the National Center for Biotechnology Information under the accession number GSE114918. Human samples re-analyzed from the Nichterwitz study[9] are under accession number GSE76514 and mouse adult single cells[8] can be accessed at GSE76381. Previous human microarray studies used to verify SNc stable gene expression were accessed from the European repository ArrayExpress (E-MEXP-1416)[10] or raw data requested to Dr. Kai C. Sonntag[12].

Figure legends

Fig. 1 Random pooling analysis identify stable genes specific for the human SNc and VTA. **a**, Hierarchical clustering of samples from the current study (18 male subjects, 74 DEGs). **b**, Identified 74-DEGs also separate SNc and VTA samples (3 female subjects) from Nichterwitz et al., 2016. **c**, Venn-diagram of the DEGs between SNc and VTA found independently for each dataset. **d**, Schematic of the algorithm used to identify stable genes, see methods. **e, f** Output of the algorithm showing the probability to find stable genes for the SNc (**e**) and VTA (**f**) as a function of sample size. For each subtype, genes with an asterisk (*) are common with overlapping DEGs (Venn-diagram in **c**). **g,** SNc and VTA stable genes segregate both dopamine neuron subtypes shown in a clustered heat map.

Fig. 2 Comparison of stable genes defining the SNc and VTA dopamine neurons in mouse and human. **a, b** Identification of SNc (**a**) and VTA (**b**) stable genes in the mouse dataset (La

Manno et. al, 2016)[8] using the random pooling algorithm (see methods and **S Fig. 3c**). **c**, Venn-diagram representation showing the overlap between stable genes across mouse and human. **d-g**, PCAs for the mouse dataset[8] when using: mouse stable genes (**d**), mouse stable list after exclusion of the three common genes (**e**), human stable genes (**f**) or human stable list after exclusion of the three common genes **g**, The accuracy (Acc.) to distinguish those subpopulations is shown as a percentage value. **i-l**, Similar analysis as (**d-g**) but applied to human samples (current study and Nichterwitz et al., 2016)[9]. **h, m** The three common stable genes are sufficient to distinguish SNc and VTA samples in mouse (**h**) and human (**m**).

Fig. 3 Identification and validation of cross-species SNc and VTA dopamine neuron predictive genes. a, Ranked mean accuracy for individual human stable genes, resolving the mouse dataset (La Manno et al., 2016)[8], upon random exclusion together with any other two genes. Common stable genes between mouse and human are labelled in blue, while additional genes with predictive value in the mouse are labelled in green. **b, c** *In situ* hybridization images of midbrain sections of the adult mouse (P56, Allen Brain Atlas) showing RNA expression pattern for Th (coronal in b, sagittal in c), the common markers Serpine2, Zcch12 and Cdh13 (in blue, b) and human stable genes with predictive value in the mouse (green, c), in addition to the mouse VTA stable marker Calb1 also useful for human (see S Fig. 4a). **d**, Immunohistochemistry on sections of human midbrain tissue confirmed differential gene expression at the protein level for the stable markers ATP2A3 (SNc), CRYM (VTA) and the mouse VTA stable gene CALB1. Scale bars: (**b,c**) 1mm for Th and 200µm for remaining markers (**d**) 50µm for all 3 pannels.

References

1 Ganat, Y. M. *et al.* Identification of embryonic stem cell-derived midbrain dopaminergic neurons for engraftment. *J Clin Invest* **122**, 2928-2939, doi:10.1172/JCI58767 (2012).

2 Kriks, S. *et al.* Dopamine neurons derived from human ES cells efficiently engraft in animal models of Parkinson's disease. *Nature* **480**, 547-551, doi:10.1038/nature10648 (2011).

3 Thompson, L., Barraud, P., Andersson, E., Kirik, D. & Bjorklund, A. Identification of dopaminergic neurons of nigral and ventral tegmental area subtypes in grafts of fetal ventral mesencephalon based on cell morphology, protein expression, and efferent projections. *J Neurosci* **25**, 6467-6477, doi:10.1523/JNEUROSCI.1676-05.2005 (2005).

4 Grimm, J., Mueller, A., Hefti, F. & Rosenthal, A. Molecular basis for catecholaminergic neuron diversity. *Proceedings of the National Academy of Sciences of the United States of America* **101**, 13891-13896, doi:10.1073/pnas.0405340101 (2004).

5 Greene, J. G., Dingledine, R. & Greenamyre, J. T. Gene expression profiling of rat midbrain dopamine neurons: implications for selective vulnerability in parkinsonism. *Neurobiology of disease* **18**, 19-31, doi:10.1016/j.nbd.2004.10.003 (2005).

6 Bifsha, P., Yang, J., Fisher, R. A. & Drouin, J. Rgs6 is required for adult maintenance of dopaminergic neurons in the ventral substantia nigra. *PLoS genetics* **10**, e1004863, doi:10.1371/journal.pgen.1004863 (2014).
7 Chung, C. Y. *et al.* Cell type-specific gene expression of midbrain dopaminergic neurons reveals molecules involved in their vulnerability and protection. *Human molecular genetics* **14**, 1709-1725, doi:10.1093/hmg/ddi178 (2005).
8 La Manno, G. *et al.* Molecular Diversity of Midbrain Development in Mouse, Human, and Stem Cells. *Cell* **167**, 566-580 e519, doi:10.1016/j.cell.2016.09.027 (2016).
9 Nichterwitz, S. *et al.* Laser capture microscopy coupled with Smart-seq2 for precise spatial transcriptomic profiling. *Nature communications* **7**, 12139, doi:10.1038/ncomms12139 (2016).
10 Cantuti-Castelvetri, I. *et al.* Effects of gender on nigral gene expression and parkinson disease. *Neurobiology of disease* **26**, 606-614, doi:10.1016/j.nbd.2007.02.009 (2007).
11 Poulin, J. F. *et al.* Defining midbrain dopaminergic neuron diversity by single-cell gene expression profiling. *Cell reports* **9**, 930-943, doi:10.1016/j.celrep.2014.10.008 (2014).
12 Simunovic, F. *et al.* Gene expression profiling of substantia nigra dopamine neurons: further insights into Parkinson's disease pathology. *Brain : a journal of neurology* **132**, 1795-1809, doi:10.1093/brain/awn323 (2009).
13 Nichterwitz, S., Benitez, J. A., Hoogstraaten, R., Deng, Q. & Hedlund, E. LCM-Seq: A Method for Spatial Transcriptomic Profiling Using Laser Capture Microdissection Coupled with PolyA-Based RNA Sequencing. *Methods in molecular biology* **1649**, 95-110, doi:10.1007/978-1-4939-7213-5_6 (2018).
14 Ramskold, D., Wang, E. T., Burge, C. B. & Sandberg, R. An abundance of ubiquitously expressed genes revealed by tissue transcriptome sequence data. *PLoS Comput Biol* **5**, e1000598, doi:10.1371/journal.pcbi.1000598 (2009).
15 Comley, L. *et al.* Motor neurons with differential vulnerability to degeneration show distinct protein signatures in health and ALS. *Neuroscience* **291**, 216-229, doi:10.1016/j.neuroscience.2015.02.013 (2015).
16 Waters, J. C. Accuracy and precision in quantitative fluorescence microscopy. *The Journal of cell biology* **185**, 1135-1148, doi:10.1083/jcb.200903097 (2009).

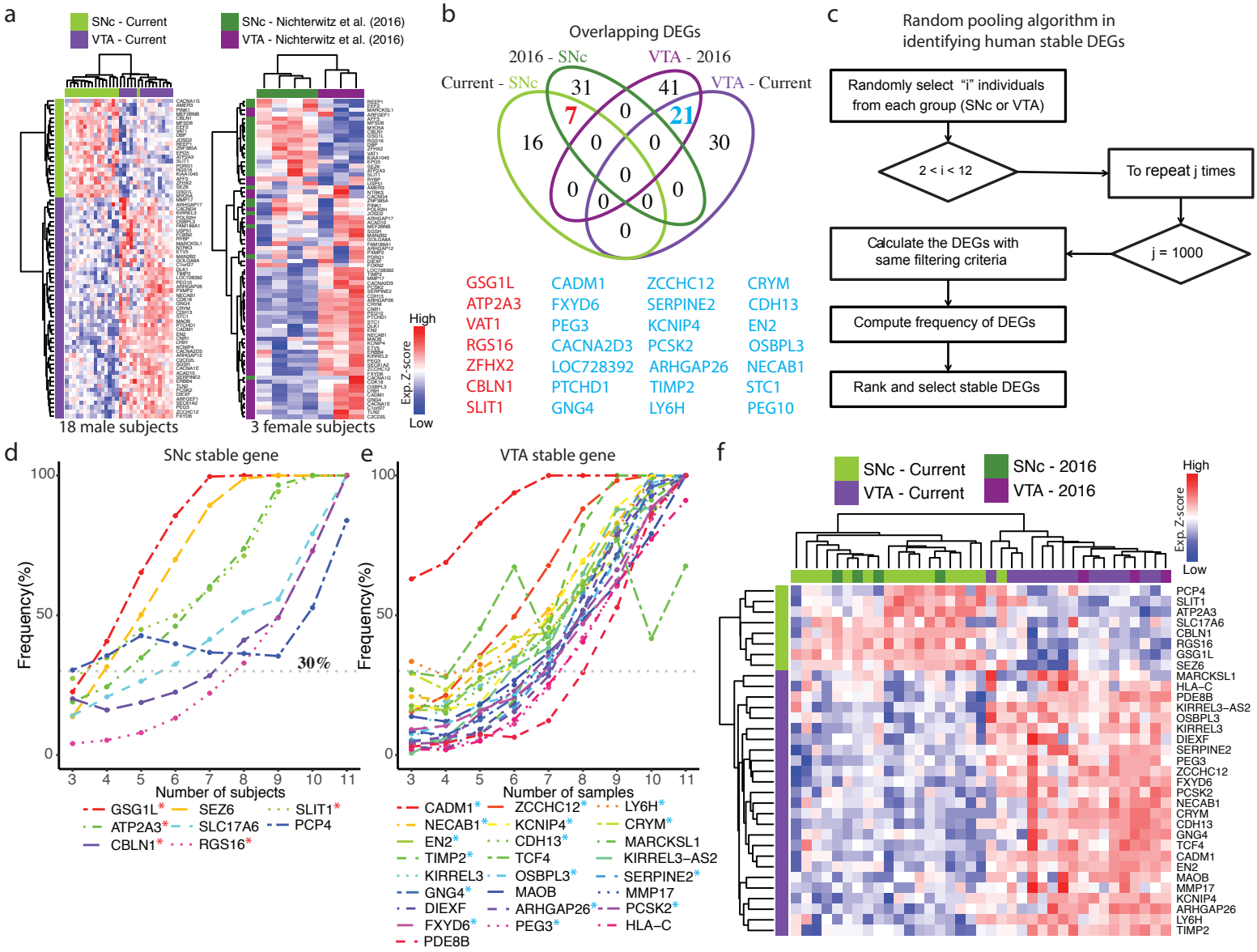
a
SNc - Current
VTA - Current
SNc - Nichterwitz et al. (2016)
VTA - Nichterwitz et al. (2016)
High
Exp. Z-score
Low
18 male subjects
3 female subjects
b
Overlapping DEGs
2016 - SNc
VTA - 2016
Current - SNc
VTA - Current
31
41
7
21
16
30
0
GSG1L
ATP2A3
VAT1
RGS16
ZFHX2
CBLN1
SLIT1
CADM1
FXYD6
PEG3
CACNA2D3
LOC728392
PTCHD1
GNG4
ZCCHC12
SERPINE2
KCNIP4
ARHGAP26
TIMP2
LY6H
CRYM
CDH13
EN2
OSBPL3
NECAB1
STC1
PEG10
c
Random pooling algorithm in identifying human stable DEGs
Randomly select "i" individuals from each group (SNc or VTA)
2 < i < 12
To repeat j times
j = 1000
Calculate the DEGs with same filtering criteria
Compute frequency of DEGs
Rank and select stable DEGs
d
SNc stable gene
Frequency(%)
100
50
0
30%
3 4 5 6 7 8 9 10 11
Number of subjects
GSG1L*
SEZ6
SLIT1*
ATP2A3*
SLC17A6
PCP4
CBLN1*
RGS16*
e
VTA stable gene
Frequency(%)
100
50
0
3 4 5 6 7 8 9 10 11
Number of samples
CADM1*
ZCCHC12*
LY6H*
NECAB1*
KCNIP4*
CRYM*
EN2*
CDH13*
MARCKSL1
TIMP2*
TCF4
KIRREL3–AS2
KIRREL3
OSBPL3*
SERPINE2*
GNG4*
MAOB
MMP17
DIEXF
ARHGAP26*
PCSK2*
FXYD6*
PEG3*
HLA–C
PDE8B
f
SNc - Current
VTA - Current
SNc - 2016
VTA - 2016
High
Exp. Z-score
Low
PCP4
SLIT1
ATP2A3
SLC17A6
CBLN1
RGS16
GSG1L
SEZ6
MARCKSL1
HLA–C
PDE8B
KIRREL3–AS2
OSBPL3
KIRREL3
DIEXF
SERPINE2
PEG3
ZCCHC12
FXYD6
PCSK2
NECAB1
CRYM
CDH13
GNG4
TCF4
CADM1
EN2
MAOB
MMP17
KCNIP4
ARHGAP26
LY6H
TIMP2

Figure 1

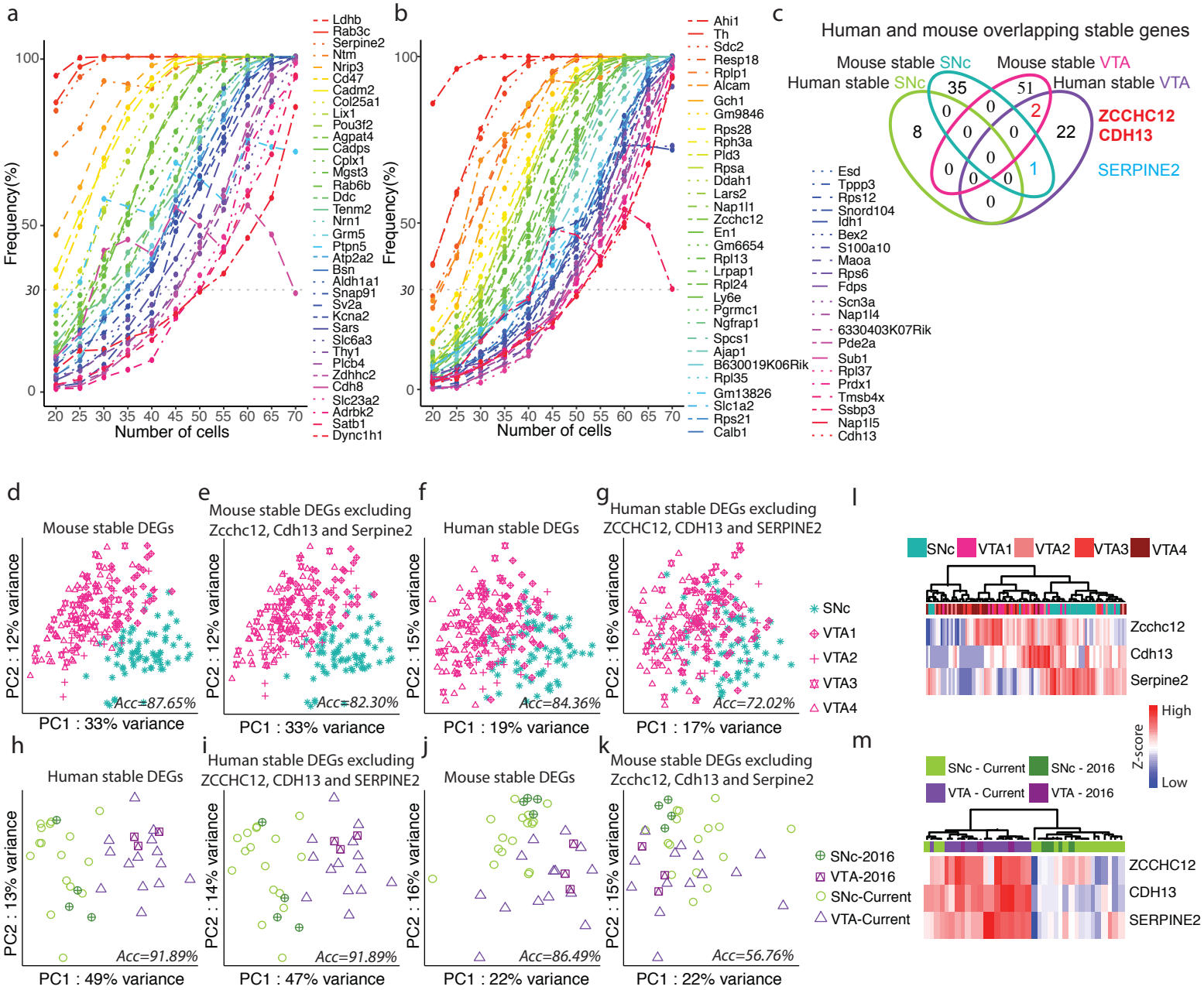
a
Frequency(%)
Number of cells
Ldhb
Rab3c
Serpine2
Ntm
Nrip3
Cd47
Cadm2
Col25a1
Lix1
Pou3f2
Agpat4
Cadps
Cplx1
Mgst3
Rab6b
Ddc
Tenm2
Nrn1
Grm5
Ptpn5
Atp2a2
Bsn
Aldh1a1
Snap91
Sv2a
Kcna2
Sars
Slc6a3
Thy1
Plcb4
Zdhhc2
Cdh8
Slc23a2
Adrbk2
Satb1
Dync1h1
b
Ahi1
Th
Sdc2
Resp18
Rplp1
Alcam
Gch1
Gm9846
Rps28
Rph3a
Pld3
Rpsa
Ddah1
Lars2
Nap1l1
Zcchc12
En1
Gm6654
Rpl13
Lrpap1
Rpl24
Ly6e
Pgrmc1
Ngfrap1
Spcs1
Ajap1
B630019K06Rik
Rpl35
Gm13826
Slc1a2
Rps21
Calb1
c
Human and mouse overlapping stable genes
Mouse stable SNc
Mouse stable VTA
Human stable SNc
Human stable VTA
ZCCHC12
CDH13
SERPINE2
Esd
Tppp3
Rps12
Snord104
Idh1
Bex2
S100a10
Maoa
Rps6
Fdps
Scn3a
Nap1l4
6330403K07Rik
Pde2a
Sub1
Rpl37
Prdx1
Tmsb4x
Ssbp3
Nap1l5
Cdh13
d
Mouse stable DEGs
PC2 : 12% variance
PC1 : 33% variance
Acc=87.65%
e
Mouse stable DEGs excluding Zcchc12, Cdh13 and Serpine2
PC2 : 12% variance
PC1 : 33% variance
Acc=82.30%
f
Human stable DEGs
PC2 : 15% variance
PC1 : 19% variance
Acc=84.36%
g
Human stable DEGs excluding ZCCHC12, CDH13 and SERPINE2
PC2 : 16% variance
PC1 : 17% variance
Acc=72.02%
SNc
VTA1
VTA2
VTA3
VTA4
h
Human stable DEGs
PC2 : 13% variance
PC1 : 49% variance
Acc=91.89%
i
Human stable DEGs excluding ZCCHC12, CDH13 and SERPINE2
PC2 : 14% variance
PC1 : 47% variance
Acc=91.89%
j
Mouse stable DEGs
PC2 : 16% variance
PC1 : 22% variance
Acc=86.49%
k
Mouse stable DEGs excluding Zcchc12, Cdh13 and Serpine2
PC2 : 15% variance
PC1 : 22% variance
Acc=56.76%
SNc-2016
VTA-2016
SNc-Current
VTA-Current
l
SNc
VTA1
VTA2
VTA3
VTA4
Zcchc12
Cdh13
Serpine2
High
Z-score
Low
m
SNc - Current
SNc - 2016
VTA - Current
VTA - 2016
ZCCHC12
CDH13
SERPINE2

Figure 2

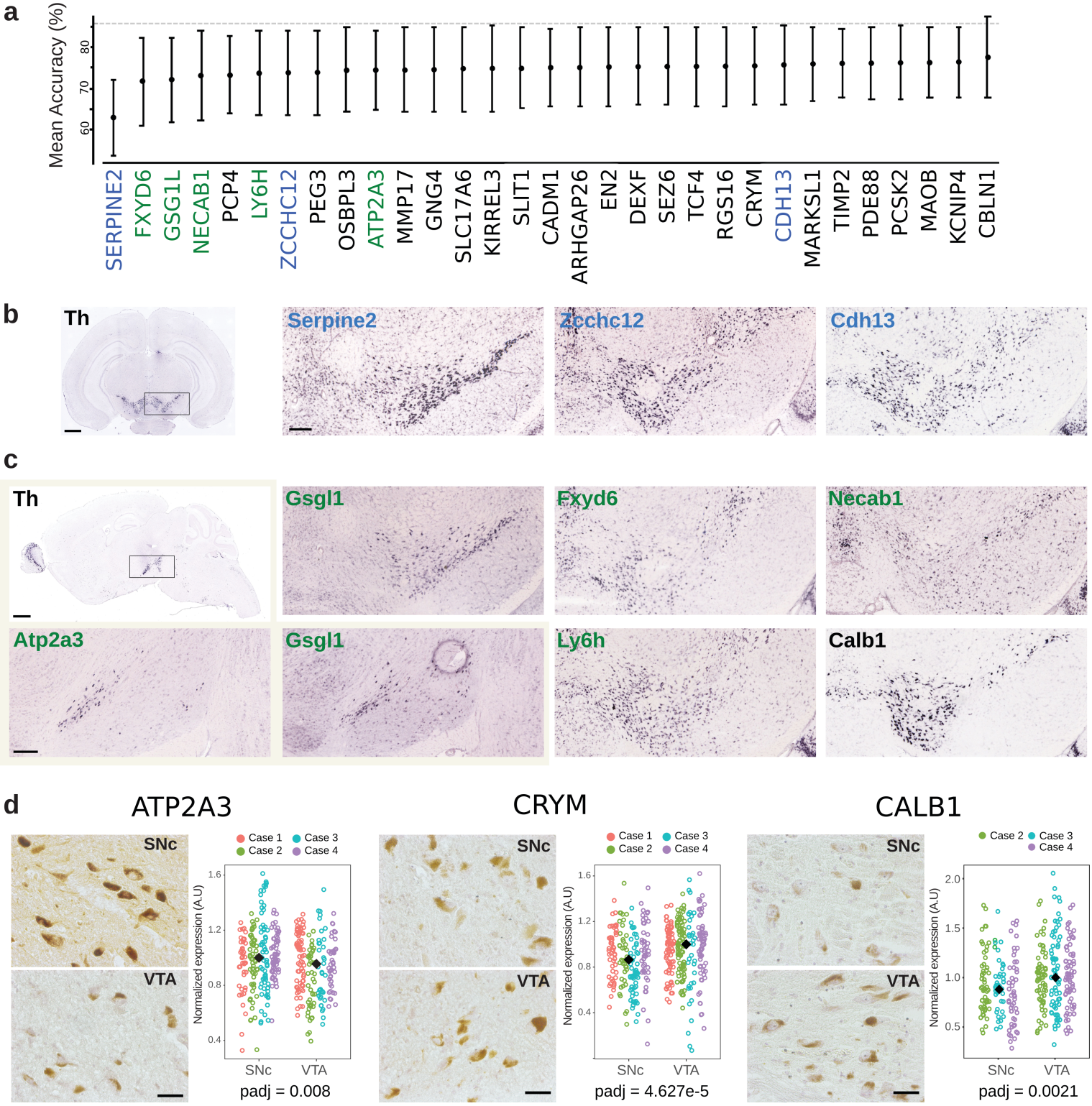
a
Mean Accuracy (%)
60
70
80
SERPINE2
FXYD6
GSG1L
NECAB1
PCP4
LY6H
ZCCHC12
PEG3
OSBPL3
ATP2A3
MMP17
GNG4
SLC17A6
KIRREL3
SLIT1
CADM1
ARHGAP26
EN2
DEXF
SEZ6
TCF4
RGS16
CRYM
CDH13
MARKSL1
TIMP2
PDE88
PCSK2
MAOB
KCNIP4
CBLN1
b
Th
Serpine2
Zcchc12
Cdh13
c
Th
Gsgl1
Fxyd6
Necab1
Atp2a3
Gsgl1
Ly6h
Calb1
d
ATP2A3
CRYM
CALB1
SNc
VTA
Case 1
Case 2
Case 3
Case 4
Normalized expression (A.U)
padj = 0.008
padj = 4.627e-5
padj = 0.0021

Figure 3